Inorg. Chem. **2003**, *42*, 3738–3750

Multidimensional Frameworks Assembled from Silver(I) Coordination Polymers Containing Flexible Bis(thioquinolyl) Ligands: Role of the Intra- and Intermolecular Aromatic Stacking Interactions

Chun-Long Chen,[†] Cheng-Yong Su,*[,†] Yue-Peng Cai,[†] Hua-Xin Zhang,[†] An-Wu Xu,[†] Bei-Sheng Kang,*[,†,‡] and Hans-Conrad zur Loye*[,§]

School of Chemistry and Chemical Engineering, Zhongshan University, Guangzhou 510275, China, State Key Laboratory of Organometallic Chemistry, Chinese Academy of Sciences, Shanghai 200032, China, and Department of Chemistry and Biochemistry, The University of South Carolina, Columbia, South Carolina 29208

Received January 30, 2003

The two flexible multidentate ligands 1,3-bis(8-thioquinolyl)propane (C3TQ) and 1,4-bis(8-thioquinolyl)butane (C4TQ) were reacted with AgX ($X = CF_3SO_3^-$ or ClO_4^-) to give four new complexes: $\{[Ag(C3TQ)](ClO_4)\}_n$ **1**, $\{[Ag(C3TQ)](CF_3SO_3)\}_n$ **2**, $\{[Ag_2(C4TQ)(CF_3SO_3)(CH_3CN)](CF_3SO_3)\}_n$ **3**, and $\{[Ag(C4TQ)](ClO_4)\}_n$ **4**. All complexes have been characterized by elemental analysis, IR, and ^1H NMR spectroscopy. Single-crystal X-ray analysis showed that chain structures form for all complexes in which the quinoline rings interact via various intra- (**1**) or intermolecular (**2**, **3**, and **4**) $\pi-\pi$ aromatic stacking interactions, which in the latter cases results in multidimensional structures. Additional weak interactions, such as Ag···O and Ag···S contacts and C–H···O hydrogen bonding, are also present and help form stable, crystalline materials. It was found that the $(CH_2)_n$ spacers ($n = 3$ or 4) affect the orientation of the two terminal quinolyl rings, thereby significantly influencing the specific framework structure that forms. If the same ligand is used, on the other hand, then the different counteranions have the greatest effect on the final structure.

Introduction

The rational design of supramolecular polymeric architectures has attracted considerable interest by chemists, not only because of their intrinsic aesthetic appeal, but also because of their potentially exploitable properties.[1] The past decade has witnessed a large number of supramolecular assemblies, including one-dimensional (1D) ladders, waves, and helices;[2,3] two-dimensional (2D) square and rectangular grids, brick walls, and nets;[4] and three-dimensional (3D) networks such as diamondoid and zeolite architectures,[5] which have been synthesized by a combination of covalent bond formation and supramolecular interactions, including hydrogen bonding, $\pi-\pi$ stacking, and M···X (X = S, O, I) contacts. As an important type of supramolecular force, $\pi-\pi$

* To whom correspondence should be addressed. E-mail: suchengyong1@yahoo.com (C.Y.S.); zurloye@mail.chem.sc.edu (H.-C.z.L.). Fax: (803) 777-8508.

† Zhongshan University.

‡ Chinese Academy of Sciences.

§ University of South Carolina.

(1) (a) Zaworotko, M. J.; Moulton, B. *Chem. Rev.* **2001**, *101*, 1629. (b) Eddaoudi, M.; Moler, D. B.; Li, H.; Chen, B.; Reineke, T. M.; Keeffe, M. O.; Yaghi, O. M. *Acc. Chem. Res.* **2001**, *34*, 319. (c) Hagrman, P. J.; Hagrman, D.; Zubieta, J. *Angew. Chem., Int. Ed.* **1999**, *38*, 2638. (d) Nomiya, K.; Yokoyama, H. *J. Chem. Soc., Dalton Trans.* **2002**, 2483.

(2) (a) Xie, Y. S.; Liu, Q. L.; Jiang, H.; Du, C. X.; Xu, X. L.; Yu, M. G.; Zhu, Y. *New J. Chem.* **2002**, *26*, 176. (b) Gamez, P.; Hoog, P. D.; Roubeau, O.; Lutz, M.; Driessen, W. L.; Spek, A. L.; Reedijk, J. *Chem. Commun.* **2002**, 1488. (c) Hong, M. C.; Zhao, Y. J.; Su, W.; Cao, R.; Fujita, M.; Zhou, Z. Y.; Chan, A. S. C. *Angew. Chem., Int. Ed.* **2000**, *39*, 2468. (d) Yaghi, O. M.; Li, H.; Groy, T. L. *Inorg. Chem.* **1997**, *36*, 4292. (e) Cui, Y.; Ngo, H. L.; Lin, W. B. *Inorg. Chem.* **2002**, *41*, 1033.

(3) (a) Guo, D.; He, C.; Duan, C.-Y.; Qian, C.-Q.; Meng, Q.-J. *New J. Chem.* **2002**, *26*, 796. (b) Fraser, C. S. A.; Eisler, D. J.; Jennings, M. C.; Puddephatt, R. J. *Chem. Commun.* **2002**, 1124. (c) Fang, C.-J.; Duan, C.-Y.; Guo, D.; He, C.; Meng, Q.-J.; Wang, Z.-M.; Yan, C.-H. *Chem. Commun.* **2001**, 2540. (d) Chen, X.-M.; Liu, G.-F. *Chem.—Eur. J.* **2002**, *8*, 4811. (e) Custelcean, R.; Ward, M. D. *Angew. Chem., Int. Ed.* **2002**, *41*, 1724. (f) Beauchamp, D. A.; Loeb, S. J. *Chem. Commun.* **2002**, 2484.

(4) (a) Biradha, K.; Hongo, Y.; Fujita, M. *Angew. Chem., Int. Ed.* **2002**, *41*, 3395. (b) Tong, M.-L.; Zheng, S.-L.; Chen, X.-M. *Chem.—Eur. J.* **2002**, *6*, 3729. (c) Wan, S.-Y.; Fan, J.; Okamura, T.-A.; Zhu, H.-F.; Ouyang, X.-M.; Sun, W.-Y.; Ueyama, N. *Chem. Commun.* **2002**, 2520. (d) Kil, S. M.; Myunghyun, P. S. *J. Am. Chem. Soc.* **2000**, *122*, 6834. (e) Fujita, M.; Kwon, Y. J.; Sasaki, O.; Yamaguchi, K.; Ogura, K. *J. Am. Chem. Soc.* **1995**, *117*, 7287. (f) Liu, G.-F.; Ye, B.-H.; Ling, Y.-H.; Chen, X.-M. *Chem. Commun.* **2002**, 1442.

10.1021/ic0341035 CCC: $25.00
Published on Web 05/10/2003

interactions have been recognized to play critical roles in the stabilization and regulatory functions of both biological systems[6] and supramolecular constructs,[7] where they have contributed significantly to self-assembly and molecular recognition processes. Well-known examples include the base stacking in DNA and the aromatic side-chain interactions in proteins.[8] Supramolecular chemists have also taken advantage of such aromatic stacking interactions for substrate recognition or for the arrangement of complicated architectures.[7,9] However, in contrast to the better-understood hydrogen bonding, the nature and effect of aromatic stacking interactions remain a great challenge while nonetheless, at the same time, these interactions are being explored for use in both biological and synthetic supramolecular systems.[10]

Multidentate ligands with variable spacers, of the general type "chelate−spacer−chelate" that can engage in aromatic side-chain interactions, have been designed and used in numerous research groups. In this area, reports on the formation of functional supramolecules with ligands containing flexible aliphatic spacers have become increasingly abundant[11−13] as the flexibility and conformational freedom of such multifunctional ligands promise great possibilities for generating novel frameworks. In addition, of course, there exist other control parameters for modifying the network topologies that include changing the size and/or the polarity of the anion,[4d,5e,14] the length of the spacer,[11a] the pH value of the reaction solution,[15] and/or the solvent.[14] Nonetheless, even with this significant number of parameters that are under the researcher's control, the rational design and a priori prediction of supramolecular polymers with specific topology structures is still difficult because the mechanism of their formation and assembly is complicated by many subtle factors.

Our research group has investigated the construction of supramolecules using ligands with flexible spacers of types I−II[16] and also those with semirigid spacers of types III−VI[17] (Scheme 1). The variety of products resulting from the assembly of metal salts with flexible ligands is expected to be more extensive than those utilizing semirigid analogues; at the same time, their synthesis and characterization is somewhat more difficult. As a result of the latter, new structures containing flexible ligands are in general less numerous, which has prompted our interest in this work.

In our previous work, ligands of types Ia and IIa and Ag(I) ions have been successfully used to construct structures with shapes that include single-strand double helicates,[16a] polymeric 2D networks,[16d] and molecular boxes.[16b] Although in complexes formed from type IIa ligands the thio-atoms have been shown to greatly aid the formation of supra-

(5) (a) Lu, C. Z.; Wu, C. D.; Lu, S. F.; Liu, J. C.; Wu, Q. J.; Zhuang, H. H.; Huang, J. S. *Chem. Commun.* **2002**, 152. (b) Zhang, J.; Tang, Y.; Tan, M.-Y.; Liu, W.-S.; Yu, K.-B. *J. Chem. Soc., Dalton Trans.* **2002**, 823. (c) Su, C.-Y.; Yang, X.-P.; Kang, B.-S.; Mak, T. C. W. *Angew. Chem., Int. Ed.* **2001**, *40*, 1725. (d) Goodgame, D. M. L.; Grachvogel, D. A.; Willams, D. J. *J. Chem. Soc., Dalton Trans*. **2002**, 2259. (e) Du, M.; Bu, X.-H.; Guo, Y.-M.; Liu, H. *Inorg. Chem.* **2002**, *41*, 4904.

(6) (a) Kim, J. L.; Nilolov, D. B.; Burley, S. K. *Nature* **1993**, *365*, 520. (b) Kim, Y.; Geiger, J. H.; Hahn, S.; Sigler, P. B. *Nature* **1993**, *365*, 512. (c) Guckian, K. M.; Schweitzer, B. A.; Ren, R. X.-F.; Sheils, C. J.; Tahmassebi, D. C.; Kool, E. T. *J. Am. Chem. Soc.* **2000**, *122*, 2213. (d) Kirksey, T. J.; Pogue-Caley, R. R.; Frelinger, J. A.; Collins, E. J. *J. Biol. Chem.* **1999**, *274*, 37 259.

(7) (a) Ponzini, F.; Zagha, R.; Hardcastle, K.; Siegel, J. S. *Angew. Chem., Int. Ed.* **2000**, *39*, 2323. (b) Fyfe, M. C. T.; Stoddart, J. F. *Acc. Chem. Res.* **1997**, *10*, 3393. (c) Janiak, C. *J. Chem. Soc., Dalton Trans.* **2000**, 3885 and references therein.

(8) (a) Hunter, C. A. *J. Mol. Biol.* **1993**, *230*, 1025. (b) Bommarito, S.; Peyret, N.; SantaLucia, J. *Nucleic Acids Res.* **2000**, *28*, 1929. (c) Hunter, C. A.; Sanders, J. K. M. *J. Am. Chem. Soc.* **1990**, *112*, 5525.

(9) (a) Hamilton, A. D.; Van Engen, D. *J. Am. Chem. Soc.* **1987**, *109*, 5131. (b) Ma, J. C.; Dougherty, D. A. *Chem. Rev.* **1997**, *97*, 1303. (c) Endo, K.; Ezuhara, T.; Koyanagi, M.; Masuda, H.; Aoyama, Y. *J. Am. Chem. Soc.* **1997**, *119*, 499. (d) Rebek, J., Jr. *Chem. Soc. Rev.* **1996**, *25*, 255.

(10) (a) Chelli, R.; Gervasio, F. L.; Procacci, P.; Schettino, V. *J. Am. Chem. Soc.* **2002**, *124*, 6133. (b) Cubberley, M. S.; Iverson, B. *J. Am. Chem. Soc.* **2001**, *123*, 7560. (c) Adams, H.; Hunter, C. A.; Lawson, K. R.; Perkins, J.; Spey, S. E.; Urch, C. J.; Sanderson, J. M. *Chem.−Eur. J.* **2001**, *7*, 4863. (d) Kim, E.; Paliwal, S.; Wilcox, C. S. *J. Am. Chem. Soc.* **1998**, *120*, 11 192.

(11) (a) Bu, X.-H.; Chen, W.; Lu, S.-L.; Zhang, R.-H.; Liao, D.-Z.; Bu, W.-M.; Shionoya, M.; Brisse, F.; Ribas, J. *Angew. Chem., Int. Ed.* **2001**, *40*, 3201. (b) Bu, X.-H.; Weng, W.; Du, M.; Chen, W.; Li, J.-R.; Zhang, R.-H.; Zhao, L.-J. *Inorg. Chem.* **2002**, *41*, 1007. (c) Bu, X.-H.; Chen, W.; Hou, W.-F.; Du, M.; Zhang, R.-H.; Brisse, F. *Inorg. Chem.* **2002**, *41*, 3477. (d) Bu, X.-H.; Chen, W.; Du, M.; Biradha, K.; Wang, W.-Z.; Zhang, R.-H. *Inorg. Chem.* **2002**, *41*, 437. (e) Bu, X.-H.; Hou, W.-F.; Du, M.; Chen, W.; Zhang, R.-H. *Cryst. Growth Des.* **2002**, *4*, 303.

(12) (a) Plater, M. J.; Foreman, M. R. St. J.; Gelbrich, T.; Coles, S. J.; Hursthouse, M. B. *J. Chem. Soc., Dalton Trans.* **2000**, 3065. (b) Plater, M. J.; Foreman, M. R. St. J.; Howie, R. A.; Skakle, J. M. S. *Inorg. Chim. Acta* **2000**, *318*, 175. (c) Plater, M. J.; Foreman, M. R. St. J.; Gelbrich, T.; Hursthous, M. B. *Cryst. Eng.* **2001**, *4*, 319. (d) Plater, M. J.; Foreman, M. R. St. J.; Gelbrich, T.; Hursthouse, M. B. *J. Chem. Soc., Dalton Trans.* **2000**, 1995. (e) Tong, M.-L.; Wu, Y.-M.; Ru, J.; Chen, X.-M.; Chang, H.-C.; Kitagawa, S. *Inorg. Chem.* **2002**, *41*, 4846. (f) Atencio, R.; Riradha, K.; Hennigar, T. L.; Poirier, K. M.; Power, K. N.; Seward, C. M.; White, N. S.; Zaworotko, M. J. *Cryst. Eng.* **1998**, 203.

(13) (a) Duncan, P. C. M.; Goodgame, D. M. L.; Menzer, S.; Willams, D. J. *Chem. Commun.* **1996**, 2127. (b) Wu, L. P.; Yamagiwa, Y.; Kuroda-Sowa, T.; Kamikawa, T.; Munakata, M. *Inorg. Chim. Acta* **1997**, *256*, 155. (c) Ma, J.-F.; Liu, J.-F.; Xing, Y.; Jia, H.-Q.; Lin, Y.-H. *J. Chem. Soc., Dalton Trans.* **2000**, 2403. (d) van Albada, G. A.; Guijt, R. C.; Haasnoot, J. G.; Lutz, M.; Spek, A. L.; Reedijk, J. *Eur. J. Inorg. Chem.* **2000**, 121. (e) Yuchi, A.; Shiro, M.; Wada, H.; Nakagawa, G. *Bull. Chem. Soc. Jpn.* **1992**, *65*, 2275. (f) Zhang, X.; Guo, G.-C.; Zheng, F.-K.; Zhou, G.-W.; Mao, J.-G.; Dong, Z.-C.; Huang, J.-S.; Mak, T. C. W. *J. Chem. Soc., Dalton Trans.* **2002**, 1334. (g) Lee, E. W.; Kim, Y. J.; Jung, D.-Y. *Inorg. Chem.* **2002**, *41*, 501.

(14) Blake, A. J.; Champness, N. R.; Cooke, P. A.; Nicolson, J. E. B.; Wilson, C. *J. Chem. Soc., Dalton Trans.* **2000**, 3811.

(15) Du, M.; Bu, X. H.; Guo, Y. M.; Ribas, J.; Diaz, C. *Chem. Commun.* **2002**, 2550.

(16) (a) Cai, Y.-P.; Zhang, H.-X.; Xu, A.-W.; Su, C.-Y.; Chen, C.-L.; Liu, H.-Q.; Zhang, L.; Kang, B.-S. *J. Chem. Soc., Dalton Trans.* **2001**, 2429. (b) Su, C. Y.; Liao, S.; Zhu, H. L.; Kang, B. S.; Chen, X. M.; Liu, H. Q. *J. Chem. Soc., Dalton Trans*. **2000**, 1985. (c) Su, C.-Y.; Liao, S.; Cai, Y.-P.; Zhang, C.; Kang, B.-S.; Liu, H.-Q. *Transition Met. Chem.* **2000**, *25*, 594. (d) Liao, S.; Su, C.-Y.; Yeung, C.-H.; Xu, A.-W.; Zhang, H.-X.; Liu, H.-Q. *Inorg. Chem. Commun.* **2000**, *3*, 405.

(17) (a) Liao, S.; Su, C.-Y.; Zhang, Z.-F.; Liu, H.-Q.; Zhu, H.-L. *Acta Crystallogr., Sect. C* **2000**, *56*, e348. (b) Liao, S.; Su, C.-Y.; Zhang, H.-X.; Shi, J.-L.; Zhou, Z.-Y.; Liu, H.-Q.; Chan, A. S. C.; Kang, B.-S. *Inorg. Chim. Acta* **2002**, *336*, 151. (c) Cai, Y.-P.; Su, C.-Y.; Zhang, H.-X.; Zhou, Z.-Y.; Zhu, L.-X.; Chan, A. S. C.; Liu, H.-Q.; Kang, B.-S. *Z. Anorg. Allg. Chem.* **2002**, *628*, 2321. (d) Su, C.-Y.; Cai, Y.-P.; Chen, C.-L.; Lissner, F.; Kang, B.-S.; Kaim, W. *Angew. Chem., Int. Ed.* **2002**, *41*, 3371. (e) Liu, H.-K.; Tan, H.-Y.; Cai, J.-W.; Zhou, Z.-Y.; Chan, A. S. C.; Liao, S.; Xiao, W.; Zhang, H.-X.; Yu, X.-L.; Kang, B.-S. *Chem. Commun.* **2001**, 1008. (f) Liu, H.-K.; Sun, W.-Y.; Tang, W.-X.; Tan, H.-Y.; Zhang, H.-X.; Tong, Y.-X.; Lan, X.; Kang, B.-S. *J. Chem. Soc., Dalton Trans.* **2002**, 3886. (g) Su, C.-Y.; Cai, Y.-P.; Chen, C.-L.; Zhang, H.-X.; Kang, B.-S. *J. Chem. Soc., Dalton Trans.* **2001**, 359. (h) Liu, J.; Tan, H.-Y.; Cai, Y.-P.; Liu, H.-K.; Su, C.-Y.; Xiao, W.; Xu, A.-W.; Kang, B.-S. *Acta Chim. Sin.* **2001**, *12*, 2209. (i) Liu, J.; Liu, H.-K.; Feng, X.-L.; Zhang, H.-X.; Zhou, Z.-Y.; Chan, A. S. C.; Kang, B.-S. *Inorg. Chem. Commun.* **2001**, *4*, 674. (j) Su, C.-Y.; Cai, Y.-P.; Chen, C.-L.; Kang, B.-S. *Inorg. Chem.* **2001**, *40*, 2210.

Scheme 1

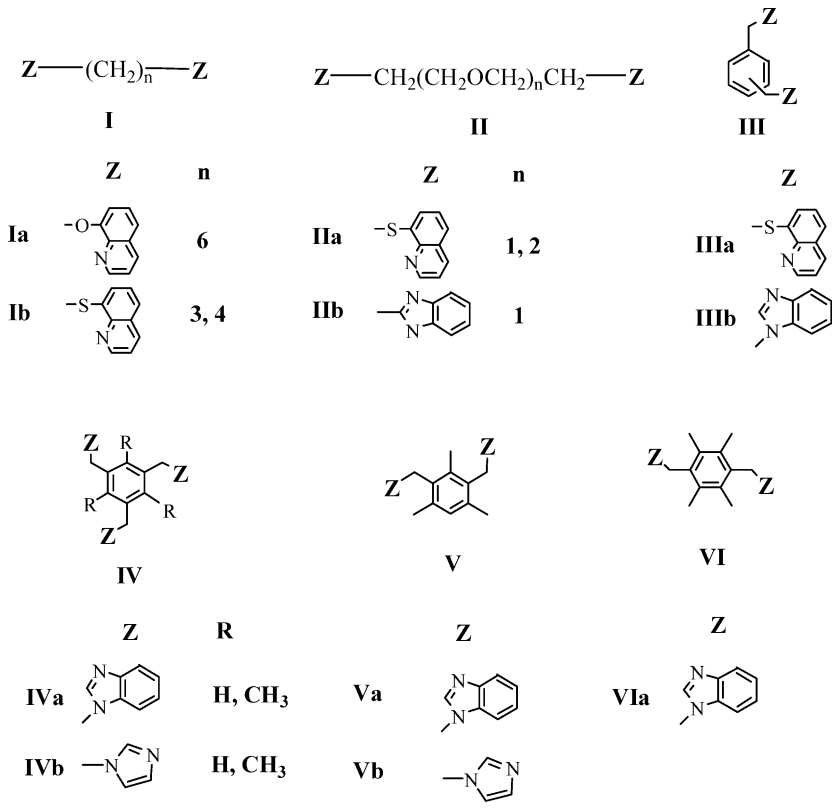

molecular architectures,[16b,d] silver complexes containing type Ib ligands are comparatively rare.[13e] As a continuation of the investigation of the effect that thioquinoline (TQ)-based ligands have on supramolecular framework structures and to study how different supramolecular polymeric architectures are influenced by $\pi-\pi$ interactions, as well as the controlling factors of the anions, we have prepared four new silver complexes, **1**−**4**, from the two ligands 1,3-bis(8-thioquinolyl)propane (C3TQ) and 1,4-bis(8-thioquinolyl)-butane (C4TQ) with variable $(CH_2)_n$ spacer length $n = 3$ and 4, respectively. Different dimensional networks for complexes **1**−**4** have resulted from $\pi-\pi$ interactions as well as from the presence of other weak intermolecular forces.

Experimental Section

General Comments. The sodium salt of 8-thioquinoline (NaTQ) was synthesized according to reported procedures.[18a] All other chemicals were of reagent grade from commercial sources and used without further purification. The C, H, N analyses were performed on a Perkin-Elmer 240 elemental analyzer. IR spectra were recorded on a Bruker EQUINOX 55 FT-IR spectrophotometer in KBr disks in the 4000−400 cm^{-1} region, and ^1H NMR spectra were recorded on an INOVA 500NB spectrometer with $SiMe_4$ as internal standard in DMSO-d_6 at room temperature.

Caution: Although we have not had trouble with the silver perchlorate used, it should be handled with appropriate precautions because perchlorate salts are known for their potential explosion hazards.

Synthesis. The ligands C3TQ and C4TQ were prepared using a modification of the previously reported synthesis.[18b] **C3TQ.** NaOH (0.50 g, 12.5 mmol) was added with stirring to a solution of NaTQ salt (1.83 g, 10 mmol) in EtOH (40 mL) at ambient temperature under N_2 and refluxed for 30 min. A solution of 1,3-dibromopropane (1.01 g, 5 mmol) in EtOH (10 mL) was added slowly over 1 h, and the resulting mixture was further refluxed for 5 h under N_2. The solid isolated from the reaction mixture after being refrigerated at 5 °C for 3 days was dissolved in $CHCl_3$ (40 mL) and washed with water. The organic layer was dried over anhydrous sodium sulfate and evaporated to dryness. The pale red powder of C3TQ was obtained in a yield of 63.7%. Calcd for $C_{21}H_{18}N_2S_2$: C, 69.58; H, 5.00; N, 7.73. Found: C, 69.46; H, 4.98; N, 7.71. IR (cm^{-1}, KBr): 3044 m, 3019 m, 2942 w, 2916 m, 1595 m, 1555 w, 1489 s, 1456 m, 1373 m, 1299 m, 1217 m, 1131 w, 1072 w, 983 s, 815 s, 781 s, 754 m, 658 m.

C4TQ. A procedure similar to that used for the synthesis of C3TQ was used, except that 1,4-dibromobutane was employed instead of 1,3-dibromopropane. The pale red powder of C4TQ was obtained in a yield of 47.8%. Calcd for $C_{22}H_{20}N_2S_2$: C, 70.18; H, 5.35; N, 7.44. Found: C, 70.25; H, 5.32; N, 7.42%. IR (cm^{-1}, KBr): 3062 w, 3031 w, 2946 m, 2922 m, 2862 m, 1596 m, 1553 m, 1487 s, 1456 s, 1359 s, 1299 s, 1216 m, 1192 m, 1149 w, 1067 m, 985 s, 821 s, 789 s, 748 s, 658 s.

Preparation of Silver(I) Complexes. All complexes were prepared by a similar procedure. A solution of the silver salt AgX (0.1 mmol, X = ClO_4^- **1**, **4**, $CF_3SO_3^-$ **2**, **3**) in CH_3CN (3 mL) was added dropwise to a stirred solution of C3TQ (18.1 mg, 0.05 mmol) or C4TQ (18.8 mg, 0.05 mmol) in $CHCl_3$ (3 mL) and the combined mixture was stirred for an additional 10 min at room temperature. Single crystals of **1**−**4** suitable for X-ray diffraction analyses were obtained by the slow diffusion of Et_2O into the clear reaction filtrate.

(18) (a) Su, C.-Y.; Li, D.-K.; Zeng, W.-Z.; Kang, B.-S. *Acta Sci. Nat. Univ. Sunyatseni* **1998**, *37*, 122. (b) Goodwin, H. A.; Lions, F. *J. Am. Chem. Soc.* **1960**, *82*, 5013.

Table 1. Crystallographic Data for Complexes **1**−**4**

	1	**2**	**3**	**4**
formula	$C_{21}H_{18}AgClN_2O_4S_2$	$C_{22}H_{18}AgF_3N_2O_3S_3$	$C_{26}H_{23}Ag_2F_6N_3O_6S_4$	$C_{44}H_{40}Ag_2Cl_2N_4O_8S_4$
fw	569.81	619.43	931.46	1167.68
space group	*P*2(1)/*c*	*Pbca*	$P\bar{1}$	*P*2(1)/*c*
T/°C	293	293	293	293
λ/Å	Mo Kα (0.71 073)	Mo Kα (0.71 073)	Mo Kα (0.71 073)	Mo Kα (0.71 073)
a/Å	13.243(7)	9.705(5)	9.781(2)	15.722(7)
b/Å	8.080(4)	18.277(10)	13.178(2)	13.768(6)
c/Å	21.019(11)	25.653(15)	13.496(3)	20.967(10)
α/°	90	90	99.231(10)	90
β/°	107.378(9)	90	110.025(11)	99.739(9)
γ/°	90	90	94.844(10)	90
V/Å^3	2146(2)	4550(4)	1595.0(6)	4473(4)
Z	4	8	2	4
μ/mm^{-1}	1.290	1.215	1.570	1.241
D_{calcd}/g cm^{-3}	1.763	1.808	1.933	1.734
R1[a]	0.0425	0.0635	0.0403	0.0651
wR2[b]	0.1157	0.1809	0.1262	0.1714

[a] $R1 = \sum||F_o| - |F_c||/\sum|F_o|$. [b] $wR2 = [\sum w(F_o^2 - F_c^2)^2/\sum w(F_o^2)^2]^{1/2}$.

{**[Ag(C3TQ)](ClO$_4$)**}$_n$ **1.** Yield: 51%. Calcd for $C_{21}H_{18}AgClN_2O_4S_2$: C, 44.26; H, 3.18; N, 4.92. Found: C, 44.17; H, 3.20; N, 4.93. IR (cm^{-1}, KBr): 3060 w, 2930 w, 1594 m, 1561 w, 1494 m, 1456 m, 1366 m, 1306 m, 1265 m, 1217 w, 1092 s, 982 m, 824 m, 777 m, 621 m.

{**[Ag(C3TQ)](CF$_3$SO$_3$)**}$_n$ **2.** Yield: 49%. Calcd for $C_{22}H_{18}AgF_3N_2O_3S_3$: C, 42.66; H, 2.93; N, 4.52. Found: C, 42.77; H, 2.94; N, 4.54. IR (cm^{-1}, KBr): 3067 w, 2939 w, 1597 w, 1562 w, 1496 m, 1454 w, 1367 w, 1273 s, 1222 m, 1155 s, 1029 s, 985 w, 831 m, 784 m, 635 s.

{**[Ag$_2$(C4TQ)(CF$_3$SO$_3$)(CH$_3$CN)](CF$_3$SO$_3$)**}$_n$ **3.** Yield: 58%. Calcd for $C_{26}H_{23}O_6N_3F_6S_4Ag_2$: C, 33.53; H, 2.49; N, 4.51. Found: C, 33.48; H, 2.48; N, 4.53. IR (cm^{-1}, KBr): 3061 w, 2941 w, 2298 w, 1594 w, 1564 w, 1495 m, 1456 w, 1372 w, 1272 s, 1239 s, 1150 s, 1027 s, 985 w, 834 m, 782 m, 635 s.

{**[Ag(C4TQ)](ClO$_4$)**}$_n$ **4.** Yield: 55%. Calcd for $C_{44}H_{40}Ag_2Cl_2N_4O_8S_4$: C, 45.26; H, 3.45; N, 4.80. Found: C, 45.33; H, 3.43; N, 4.81. IR (cm^{-1}, KBr): 3061 w, 3032 w, 2946 w, 2922 w, 1595 w, 1555 w, 1489 m, 1456 m, 1378 w, 1360 m, 1301 m, 1216 w, 1190 w, 1142 s, 1088 s, 984 m, 822 m, 787 m, 628 m.

Crystallography. Experimental details of the X-ray analysis as well as the crystallographic data are provided in Table 1. Selected bond distances and bond angles are listed in Table 2. All diffraction data were collected on a Bruker Smart 1000 CCD diffractometer with graphite-monochromated Mo Kα radiation (λ = 0.71073 Å) at room temperature using the program SMART[19] and were processed by SAINT+.[20] Absorption corrections were applied using SADABS.[21] Space groups were determined from systematic absences and further justified by the results of the refinements. In all cases, the structures were solved by direct methods and refined using the full-matrix least-squares method against F^2 with SHELXTL software.[22] All non-hydrogen atoms were refined with anisotropic displacement parameters. After that, all hydrogen atoms of the ligands were placed at idealized positions and refined as riding atoms with relative isotropic parameters of the heavy atoms to which they were attached. CCDC reference numbers CCDC 198 182−198 185.

(19) *SMART*, version 5.0; Bruker AXS: Madison, WI, 1998.
(20) *SAINT+*, version 6.0; Bruker AXS: Madison, WI, 1999.
(21) Blessing, R. *Acta Crystallogr., Sect. A* **1995**, *51*, 33.
(22) Sheldrick, G. M. *SHELX-97*: *Program for Crystal Structure Solution and Refinement*; University of Göttingen: Göttingen, Germany, 1997.

Table 2. Selected Bond Lengths (Å) and Angles (°) for Complexes **1**−**4**[a]

	Complex **1**		
Ag(1)−N(1)	2.350(4)	N(1)−Ag(1)−S(2)	103.94(10)
Ag(1)−N(2)	2.355(4)	N(2)−Ag(1)−S(2)	75.68(9)
Ag(1)−S(1)A	2.613(2)	S(1)A−Ag(1)−S(2)	112.91(4)
Ag(1)−S(2)	2.683(2)	N(1)−Ag(1)−S(1)	71.22(9)
Ag(1)−S(1)	2.815(2)	N(2)−Ag(1)−S(1)	90.11(9)
N(1)−Ag(1)−N(2)	155.42(14)	S(1)A−Ag(1)−S(1)	116.27(3)
N(1)−Ag(1)−S(1)A	103.11(11)	S(2)−Ag(1)−S(1)	130.38(5)
N(2)−Ag(1)−S(1)A	99.43(10)	C(8)−S(1)−C(10)	101.2(2)
	Complex **2**		
Ag(1)−N(1)	2.296(6)	N(2)−Ag(1)−S(2)	75.58(11)
Ag(1)−N(2)	2.305(5)	N(1)−Ag(1)−S(1)	75.79(13)
Ag(1)−S(2)	2.690(2)	N(2)−Ag(1)−S(1)	101.18(11)
Ag(1)−S(1)	2.699(2)	S(2)−Ag(1)−S(1)	175.53(5)
N(1)−Ag(1)−N(2)	174.63(17)	N(1)−Ag(1)−S(2)	107.19(13)
	Complex **3**		
Ag(1)−N(2)A	2.253(3)	N(2)A−Ag(1)−S(2)A	77.17(7)
Ag(1)−S(1)	2.423(1)	S(1)−Ag(1)−S(2)A	124.43(3)
Ag(1)−O(6)	2.478(4)	O(6)−Ag(1)−S(2)A	87.10(13)
Ag(1)−S(2)A	2.629(1)	N(1)B−Ag(2)−N(3)	88.69(14)
Ag(2)−N(1)B	2.322(3)	N(1)B−Ag(2)−S(2)	136.30 (7)
Ag(2)−N(3)	2.380(5)	N(3)−Ag(2)−S(2)	111.33(11)
Ag(2)−S(2)	2.471(1)	N(1)B−Ag(2)−S(1)B	74.35(7)
Ag(2)−S(1)B	2.662(1)	N(3)−Ag(2)−S(1)B	99.46(11)
N(2)A−Ag(1)−S(1)	150.94(7)	S(2)−Ag(2)−S(1)B	134.57(3)
N(2)A−Ag(1)−O(6)	95.55(11)	S(1)−Ag(1)−O(6)	104.07(9)
	Complex **4**		
Ag(1)−N(1)	2.323(7)	N(1)−Ag(1)−S(1)	78.74(17)
Ag(1)−N(4)	2.327(6)	N(4)−Ag(1)−S(1)	129.31(17)
Ag(1)−S(4)	2.512(3)	S(4)−Ag(1)−S(1)	128.04(7)
Ag(1)−S(1)	2.543(2)	N(2)−Ag(2)−N(3)	91.0(2)
Ag(2)−N(2)	2.374(5)	N(2)−Ag(2)−S(3)	140.08(16)
Ag(2)−N(3)	2.395(6)	N(3)−Ag(2)−S(3)	77.21(15)
Ag(2)−S(3)	2.529(2)	N(2)−Ag(2)−S(2)	77.08(15)
Ag(2)−S(2)	2.539(2)	N(3)−Ag(2)−S(2)	130.88(14)
N(1)−Ag(1)−N(4)	108.7(2)	S(3)−Ag(2)−S(2)	138.35(7)
N(1)−Ag(1)−S(4)	139.0(2)	N(4)−Ag(1)−S(4)	79.34(17)

[a] Symmetry codes for **1**: A $-x + 1$, $y - 1/2$, $-z + 3/2$. Symmetry codes for **3**: A $-x + 2$, $-y + 1$, $-z + 1$; B $x - 1$, y, z.

Results and Discussion

Syntheses. The two flexible ligands of type Ib containing $(CH_2)_n$ backbones (n = 3 C3TQ; n = 4 C4TQ) with rigid TQ as terminal-chelating groups (Scheme 1) have been employed for the syntheses of complexes **1**−**4**. Scheme 2 shows the reaction processes of type Ib ligands with silver salts AgX (X = $CF_3SO_3^-$ or ClO_4^-). It was found that the

Scheme 2

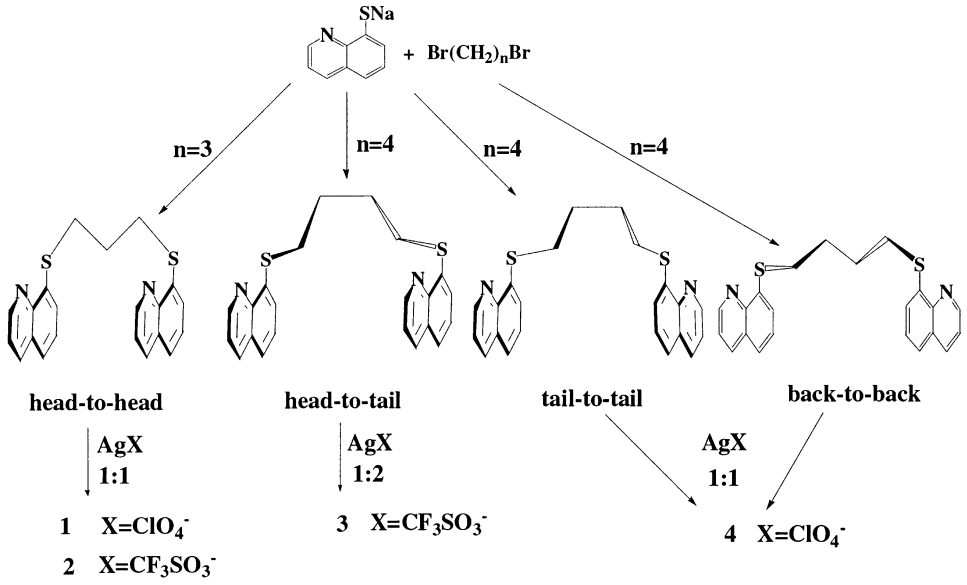

structures (see crystal structure sections) of the products correlate closely with the $(CH_2)_n$ spacer length and the different arrangements of the two quinoline rings (Q). As shown in Scheme 2, the two quinoline moieties can orient the heteroaromatic plane into head-to-head (N-rings on the same side of the backbone pointing in the same directions), head-to-tail (N-rings on two sides of the backbone pointing in the same directions), tail-to-tail (N-rings on two sides of the backbone pointing in opposite directions), or back-to-back (two Q rings coplanar pointing in opposite directions) conformations. The head-to-head conformation is found in **1** and **2** where the two Q rings take on different dihedral angles, the head-to-tail conformation is found in **3**, whereas both the tail-to-tail and back-to-back conformations coexist in **4**. Different conformations in different complexes result in entirely different aromatic stacking, which will be discussed in detail later. Unlike the helical complexes formed from OQ (oxaquinoline)-substituted type Ia ligands,[16a] the thioether atom in these ligands not only provides a potential bridging site, but also enables the complexes to form extensive aromatic stacking systems because of its preference for the gauche conformation.[16b,d,23]

Crystal Structures. $\{$**[Ag(C3TQ)](ClO$_4$)**$\}_n$ **1.** Complex **1** consists of a 1D cationic chain of AgC3TQ and ClO_4^- counteranions; the asymmetric unit of the 1D chain is shown in Figure 1. The ligand C3TQ acts as a bis-bidentate chelator to coordinate the two symmetry-related Ag atoms in a nonequivalent manner with the two S atoms functioning differently: S1 is a μ_2-bridging atom and S2 is a terminal donor. The Ag1−S1 bond is longer than the Ag1−S2 bond by 0.13 Å, whereas the Ag1−S1A bond is the shortest (2.613 Å). Each Ag atom is coordinated by two TQ moieties from two C3TQ groups in the equatorial plane with the bridging S1 in the axial positions, thus forming a distorted square pyramidal geometry of AgN_2S_3. Given the folding of the ligand at the sulfur atom (the torsion angle C8−S1−C10−C11 is 114.4°), the two quinoline rings belonging to the same ligand are nearly parallel to each other (*head-to-head*, dihedral angle 19.9°), resulting in intraligand $\pi-\pi$ interactions (centroid-to-centroid distances are in the range of 3.873(4)−4.027(4) Å) as shown in Figure 2. The eight-membered macrocyclic units composed of $Ag_2S_3C_3$ share the Ag−S edges, thus generating an infinite linear chain down the *b* axis with the interligand $\pi-\pi$ interaction (centroid-to-centroid distance 4.126(4) Å). Both types of $\pi-\pi$ stacking interactions are intramolecular, resulting in a closely packed chain structure, which precludes the possibility of forming intermolecular $\pi-\pi$ interactions. The ClO_4^- anions interact weakly with the quinoline-ring hydrogen atoms where the distances between protons and oxygens lie in the range of 2.60−2.67 Å. A closely related structure was reported for $\{[Ag(C3TQ)](NO_3)\}_n$[13e] where the counteranions also do not appear to influence the AgC3TQ chain structure.

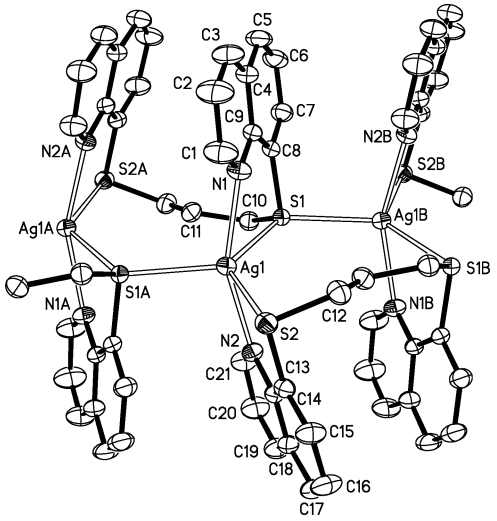

Figure 1. View of the asymmetric unit in **1** showing the metal coordination environment.

$\{$**[Ag(C3TQ)](CF$_3$SO$_3$)**$\}_n$ **2.** Complex **2** also contains a polymeric chain of AgC3TQ but with $CF_3SO_3^-$ instead of

(23) Grapperhaus, C. A.; Li, M.; Mashuta, M. S. *Chem. Commun.* **2002**, 1792 and references therein.

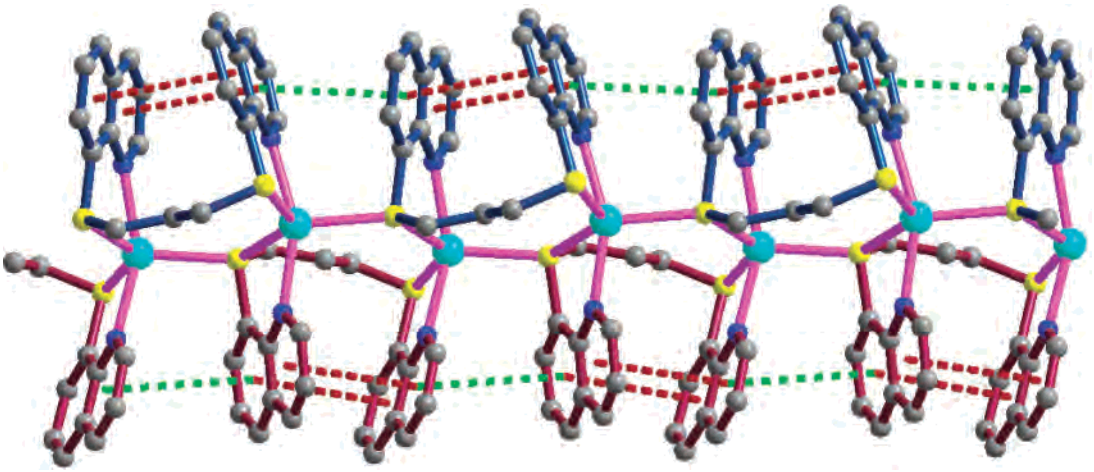

Figure 2. Linear chain along the *b* axis showing the intraligand (red) and interligand (green) $\pi-\pi$ interactions (dashed lines). Key: Ag (cyan), S (yellow), N (blue), C (gray). Ligands are distinguished by different bond colors.

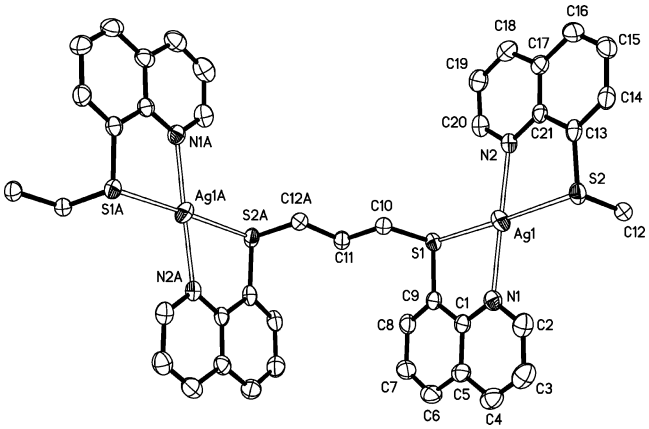

Figure 3. View of the asymmetric unit in **2** showing the metal coordination environment.

ClO_4^- counteranions. The asymmetric unit of the 1D chain is shown in Figure 3. The ligand C3TQ again acts as a bis-bidentate chelating agent to coordinate equivalently with two symmetry-related Ag atoms. Each Ag(I) atom adopts a square planar geometry, AgN_2S_2, containing two nitrogen and two sulfur atoms from the TQ moieties of the two ligands; the two Ag−N and Ag−S bonds are almost equivalent. As a result, each repeating unit in the molecule is composed of one pair of Ag(I) ions bridged by a C3TQ ligand, while another C3TQ ligand connects two such dimers together with mirror symmetry to form a 1D chain running along the crystallographic 2_1 axis in the *b* direction (Figure 4a). This arrangement of the ligand endows the chain with a helical sense (M or P as shown in Scheme 3) with a long pitch of 18.28 Å. The two TQ rings from two ligands chelating to the same Ag(I) ion are parallel to each other with a dihedral angle of only 1.7°, whereas those chelated to different Ag(I) ions are nearly perpendicular (dihedral angle 80.4°). This is caused by the gauche conformation of the sulfur atoms, which allows two TQ rings to fold up against the $(CH_2)_3$ backbone and take such an "open" head-to-head conformation, generating a trapezoidal wave chain as shown in Figure 4b. Such trapezoids provide ideal aromatic stacking interaction sites on both sides (indicated in Figure 4b), thus pulling the M and P chains together by intermolecular $\pi-\pi$ interactions (centroid-to-centroid distances are in the range of 3.537(4)−3.766(4) Å) to stack alternately into a 2D layer, as depicted in Figure 5a. At the same time, weak Ag···S (3.42−3.52 Å) interactions between the chains further strengthen the 2D layers. Finally, the $CF_3SO_3^-$ anions form weak C−H···O interactions with the quinoline-ring hydrogen atoms (the distances between protons and oxygens are in the range 2.52−2.53 Å) to fabricate a 3D network by connecting these 2D layers, as shown in Figure 6.

{[Ag_2(C4TQ)(CF_3SO_3)(CH_3CN)](CF_3SO_3)}$_n$ 3. Complex **3** is composed of an asymmetric cationic unit Ag_2C4TQ-

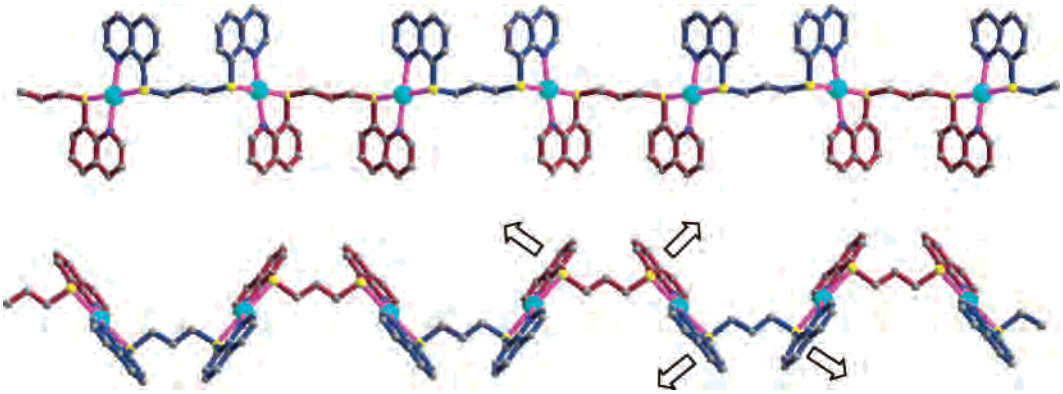

Figure 4. Chain structure in **2**: up and down arrangement of the ligands (top), trapezoidal wave pattern providing potential aromatic stacking sites indicated by arrows (bottom). Key: same as Figure 2.

Scheme 3

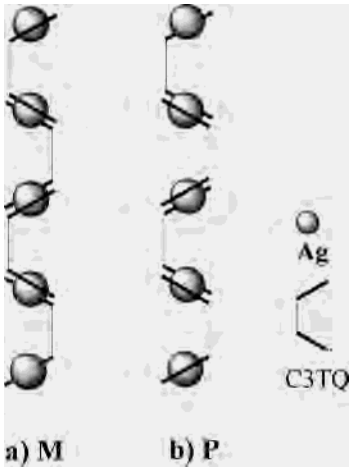

(MeCN)(CF_3SO_3) (Figure 7) and a discrete $CF_3SO_3^-$ anion. Figure 8a shows the coordination geometry of the two independent Ag(I) ions involving three ligands. Each TQ ring of the C4TQ ligand chelates one Ag(I) ion while the S atom further bridges another Ag(I) ion. The Ag1 atom is coordinated by a $CF_3SO_3^-$ anion and Ag2 is coordinated by a MeCN molecule, in addition to the chelation of one TQ moiety from one ligand and bridging by a S atom from another ligand (also see Figure 9). In this way, an eight-membered Ag_4S_4 macrocyclic ring is formed as shown in Figure 8b, which is then stretched outward in the *bc* plane by the quinoline rings and extended longitudinally along the *a* axis by the $(CH_2)_4$ spacer bridge, constructing a "double" chain as depicted in Figure 9. Both of the Ag ions are located in a distorted tetrahedral geometry. The chelating Ag−S and Ag−N bonds, respectively, for the two Ag centers resemble each other and are comparable with those in **1**, but the bridging Ag−S bond (2.471(1) Å) is significantly shorter than that (2.815(2) Å) in **1**.

A notable feature of this chain structure is that the four TQ rings are linked to each other via a cyclic Ag_4S_4 skeleton and provide potential supramolecular recognition sites for $\pi-\pi$ aromatic stacking interactions in four directions, as shown in Figures 8b and 9. A pair of ligands take the head-to-tail conformation to span across two of the Ag_4S_4 cycles in the chain, with the two TQ rings of each ligand having a dihedral angle of 12.93°. Therefore, the four TQ rings are almost coplanar, arranged orthogonally along the double chain between the $(CH_2)_4$ spacers. This arrangement makes it possible for every chain to interact with another one in four directions. The adjacent chains are zippered together by interdigitating TQ rings on both sides of the chain, thus generating 2D layers in both the *ab* and *ac* planes (see Figure S1). In fact, each chain interdigitates with four neighboring chains into a 3D porous network via multiple offset intermolecular $\pi-\pi$ interactions (centroid-to-centroid distance in the range of 3.632(2)−3.915(3) Å), as depicted in Figure 10. This creates rhombic channels with edge lengths of 9.4 Å in which the $CF_3SO_3^-$ counteranions are located and interact via weak C−H···O interactions with the quinoline-ring hydrogen atoms (the distance between protons and oxygens in the range of 2.44−2.50 Å.

{[Ag(C4TQ)][ClO_4)]}$_n$ 4. Complex **4** consists of polymeric cationic AgC4TQ chains and ClO_4^- anions, where the asymmetric $Ag_2(C4TQ)_2$ unit is shown in Figure 11. The ligand again acts as a bis-bidentate chelating agent toward two Ag(I) ions on one side of the chain while another bridging ligand chelates two Ag(I) ions on the other side, sharing one of the Ag atoms with the former. This results in an infinite zigzag chain that runs along the *b* axis, as shown

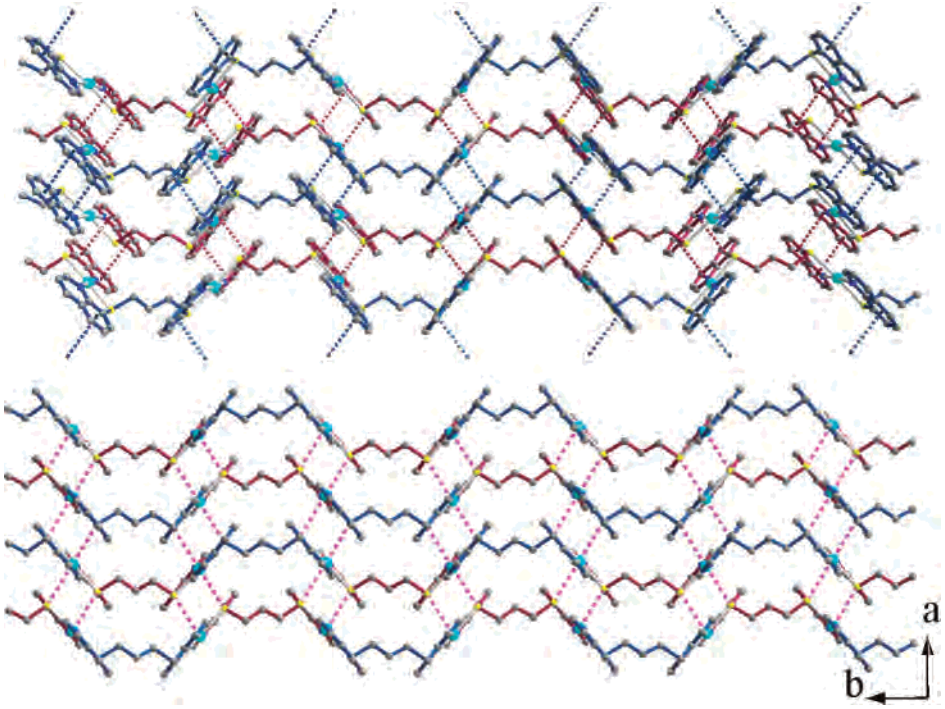

Figure 5. 2D layer formed via intermolecular $\pi-\pi$ interactions (top) and Ag···S contacts (bottom) in the *ab* plane in **2**.

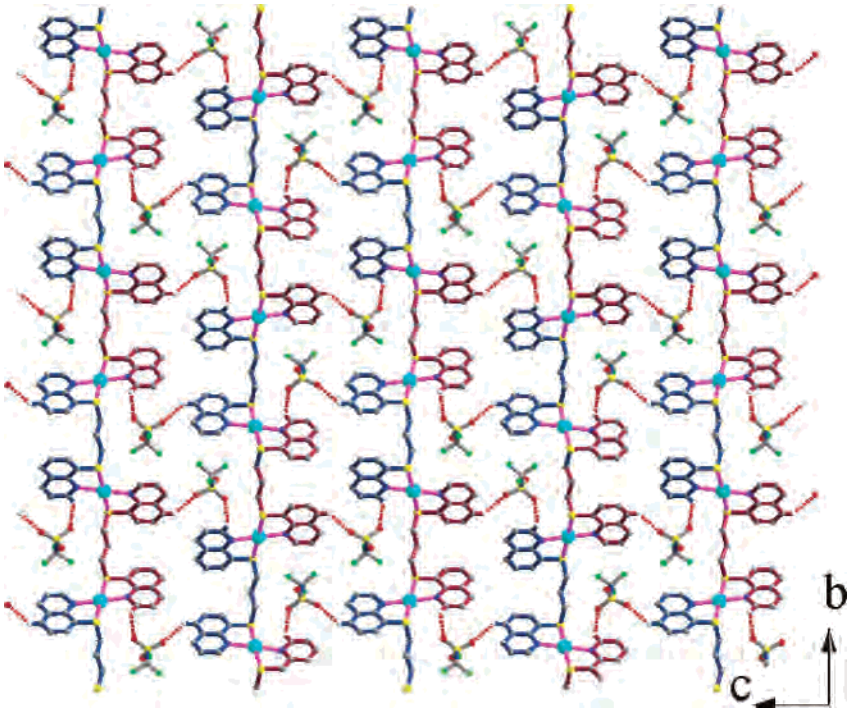

Figure 6. 2D network generated by weak O···H−C hydrogen bonding in the *bc* plane in **2**.

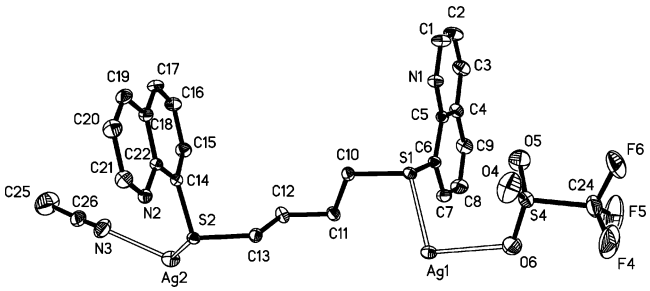

Figure 7. View of the asymmetric unit in **3**.

in Figure 12. Similar to **2**, each Ag(I) ion is coordinated by two nitrogens and two sulfurs from the TQ moieties of two ligands, but adopts a distorted tetrahedral geometry rather than a square planar one. The Ag−N bonds are slightly elongated whereas the Ag−S bonds are remarkably shortened. This difference is caused by the dissimilar conformations adopted by the ligands in **4**. As indicated in Figure 12, the ligands forming the backbone of the chain alternately take on two different conformations: one back-to-back and one tail-to-tail (Scheme 2). The TQ rings of the back-to-back conformational ligand are almost coplanar (dihedral angle 4.41°, S···S distance 5.95 Å), whereas those of the tail-to-tail one are offset (dihedral angle 11.24°, S···S distance 6.67 Å). This arrangement of the ligand results in a helical chain (Scheme 4) with a pitch of 13.78 Å comparable to **2**, but involves a different aromatic ring-stacking format.

As shown in Figures 12−14, three types of $\pi-\pi$ interactions are present: two from the tail-to-tail ligand in two directions (labeled α and β) and the third from the back-to-back ligand (labeled γ). The α-type $\pi-\pi$ interactions join a pair of P and M chains in the *a* direction, whereas the β-type $\pi-\pi$ interactions connect a pair of enantiomeric chains in the *c* direction. The γ-type $\pi-\pi$ interactions, utilizing different ligand conformations, also join a pair of helical chains in the *a* direction. Figure 13 depicts how the α and β $\pi-\pi$ interactions organize two pairs of helical chains, AB and A′B′ (A or A′, P helicate; B or B′, M helicate), via mutual aromatic stacking interactions into a quadruple-stranded arrangement along the *b* axis: A and B (or B′ and A′), which are related by glide plane, recognize each other via α interactions in the *a* direction, while A′ and B (or B′ and A), which are also glide-plane related, recognize each other via β interactions in the *c* direction. A and A′ (or B and B′) are the same-handed helical chain and are related by 2_1 symmetry. Therefore, a stacked aromatic column is formed in the center that is surrounded by these four helical chains, ABA′B′, to generate an aromatic stacking interactions unit $\alpha\beta\alpha'\beta'$, which repeats along the *c* direction. In fact, such stacked aromatic columns exist between every AB chain, thus generating a double layer AB−A′B′−AB−A′B′··· with the AB chain acting as the unit in the *bc* plane as shown in Figure 14a. On the basis of the above discussion, this double layer can be thought of as consisting of the α interaction-related AB units, which extend in the *c* direction via β interactions. A closely stacked aromatic sheet is therefore formed in the middle of the double layers, as shown in Figure 14b. In addition, the double layer also provides γ interaction sites on both sides, as indicated in Figure 14c. To simplify these interaction/structure pictures, parts d and e of Figure 14 demonstrate how the α interaction connecting AB units are in turn connected via γ interactions in the *a* direction. Therefore, a layer of AB−AB−AB−AB··· (or A′B′−A′B′−A′B′−A′B′···) extended in the *ab* plane is formed via alternate γ aromatic stacking interactions. When comparing this with the structure of **3**, the α interaction-related AB units in **4** can also be thought of as *pseudo* double chains, similar

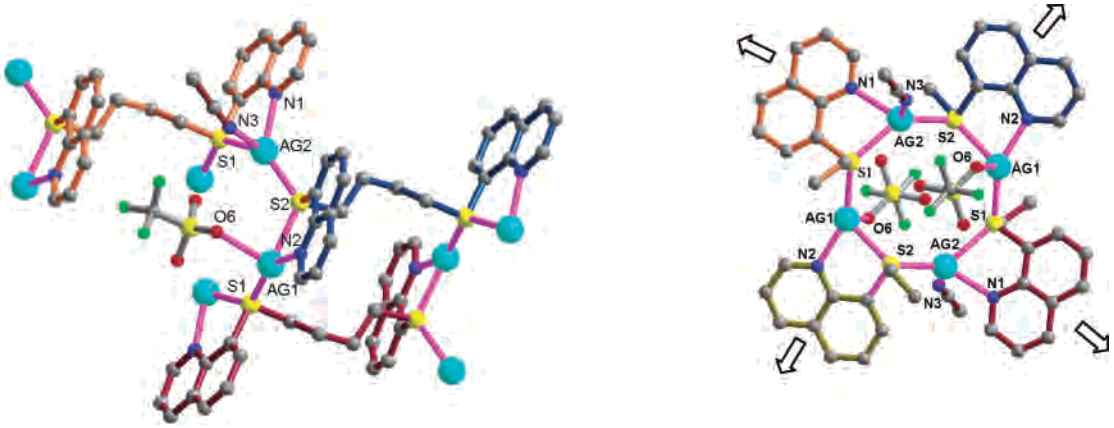

Figure 8. View of the coordination geometry for the two independent Ag(I) ions (left) and an eight-membered macrocyclic ring formed by four Ag atoms, four thioquinolines (TQ), two coordinated anions $CF_3SO_3^-$, and two coordinated CH_3CN (right) in **3**. Arrows indicate potential aromatic stacking sites. Key: same as Figure 2.

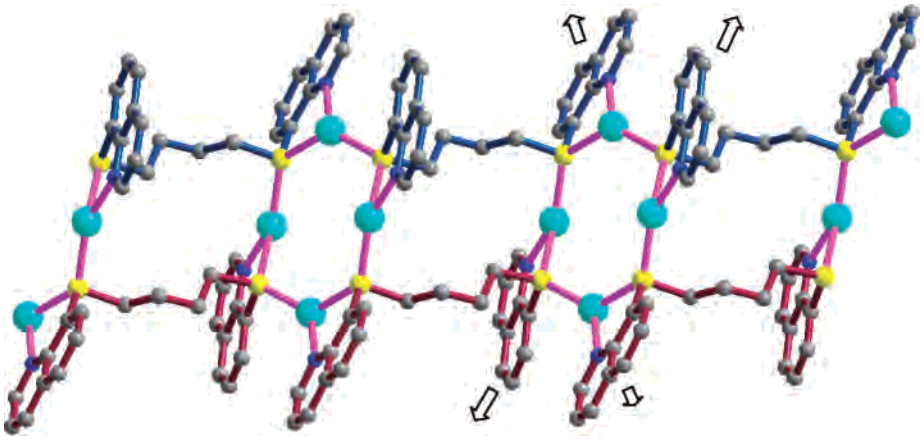

Figure 9. Double chain structure in **3** with potential aromatic stacking sites indicated by arrows. Key: same as Figure 2.

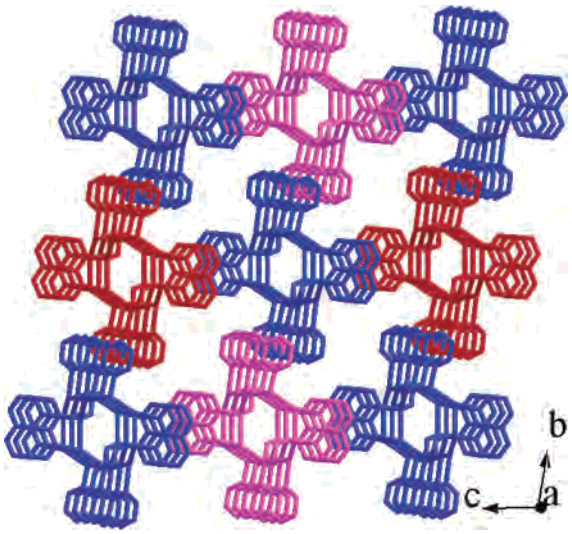

Figure 10. 3D network formed by the double chains via four directional aromatic stacking interactions in **3**.

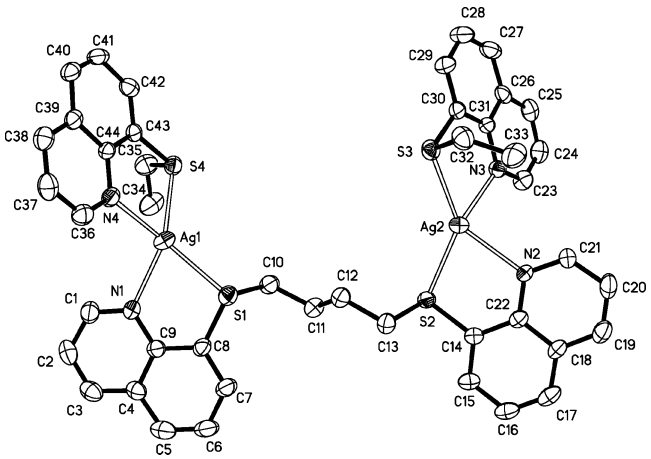

Figure 11. View of the asymmetric unit in **4**.

to those in **3**, providing $\pi-\pi$ aromatic stacking interaction sites in four directions (β interactions in *a* or opposite directions; γ interactions in *c* or opposite directions) too. The 3D network is constructed from these AB units by forming AB−A′B′−AB−A′B′··· double layers via β aromatic stacking interactions in the *bc* plane and AB−AB−AB−AB··· (or A′B′−A′B′−A′B′−A′B′···) layers via γ aromatic stacking in the *ab* plane. The multiple offset, intermolecular $\pi-\pi$ interactions that are involved are summarized in Table 3. Other weak interactions such as Ag···O_{anion} (3.36 Å) and $C_{quinoline}$−H···O_{anion} hydrogen bonding (H···O_{anion}, 2.46−2.56 Å) are also present between the layers but apparently do not significantly influence the topology of the networks.

In general, the chain structures of **1** and **3** can be regarded as "double" chains because cyclic rings are formed along the chain via the bridging S atoms. In **1**, the eight-membered

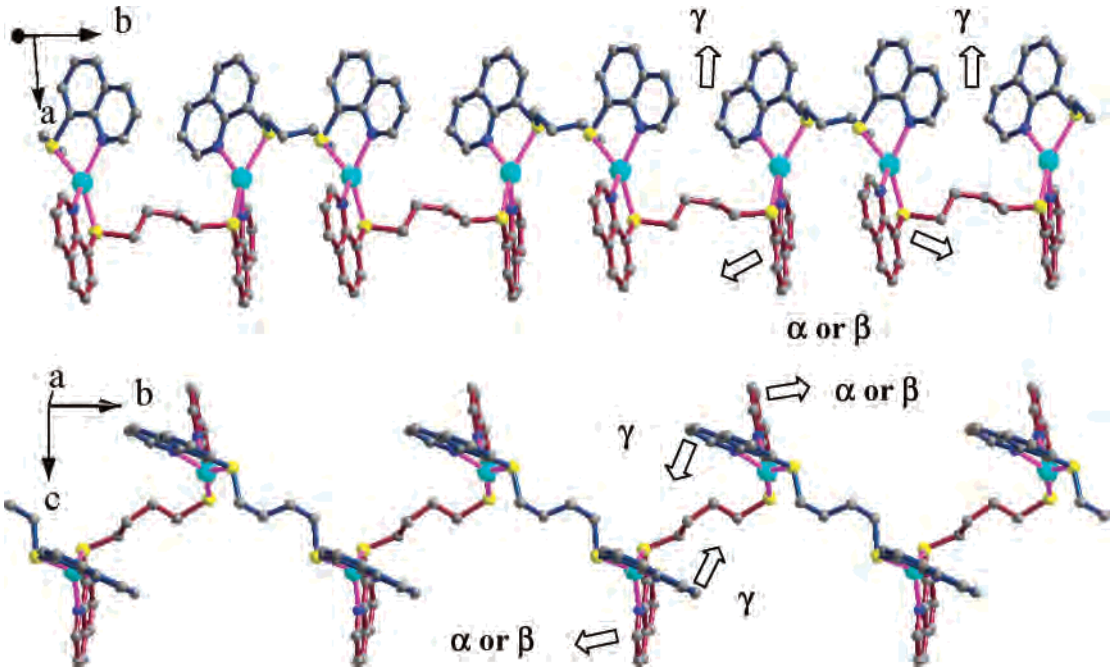

Figure 12. View of the chain structure in **4** in different directions showing two types of ligand conformations (blue, back-to-back; red, tail-to-tail). Arrows indicate potential aromatic stacking sites. Key: same as Figure 2.

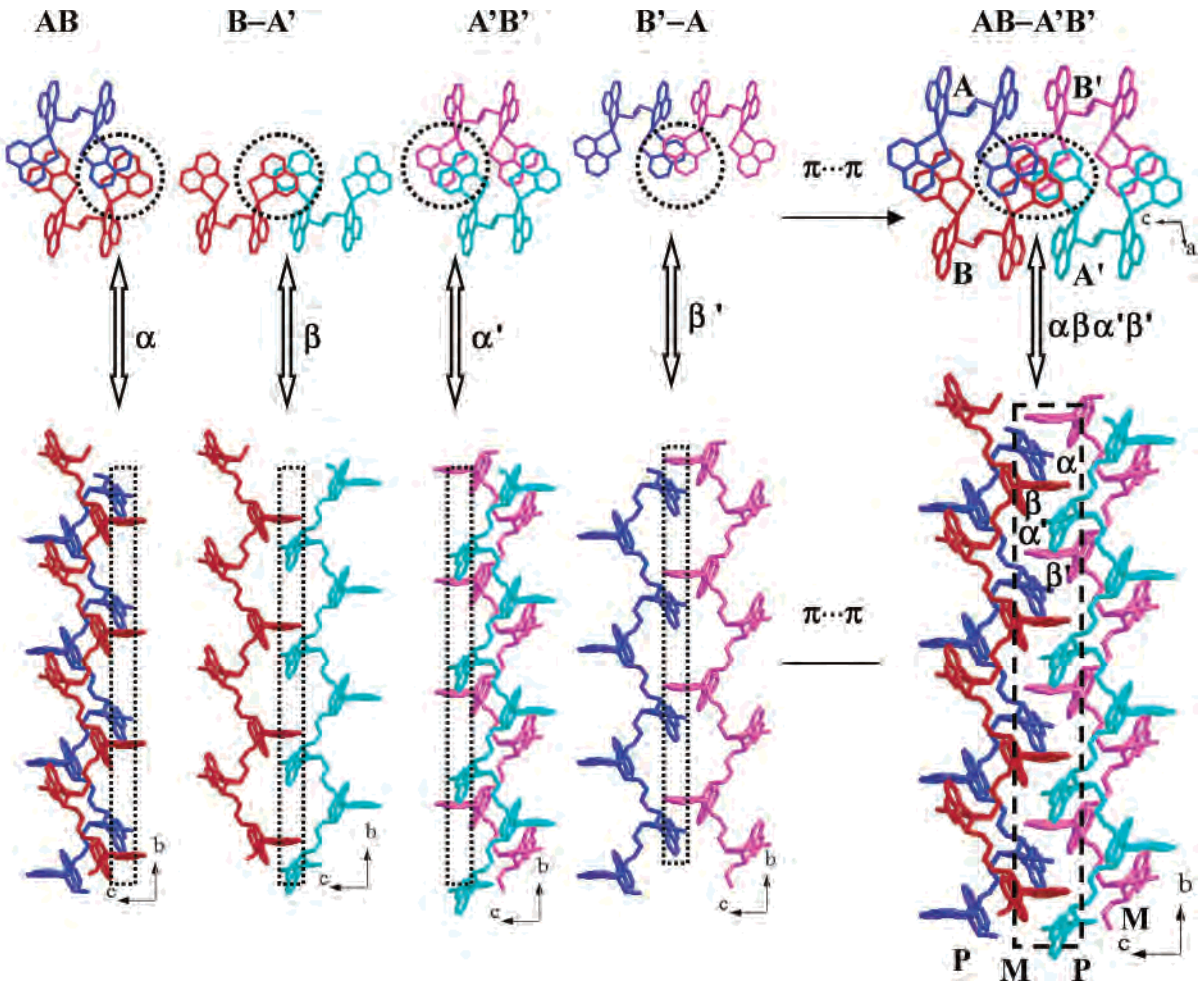

Figure 13. Perspective view (top) and side view (bottom) of the quadruple-stranded arrangement in **4** organized by α- and β-type $\pi-\pi$ interactions from two pairs of helical chains: A (blue, P) and B (red, M); A′ (cyan, P) and B′ (pink, M). The α or β interactions that formed between every two chains and the stacked aromatic column (repeating $\alpha\beta\alpha'\beta'$) that formed in the center of four chains are highlighted by dashed circles or rods. The $(CH_2)_n$ spacer of the tail-to-tail ligand is omitted for clarity in the top view.

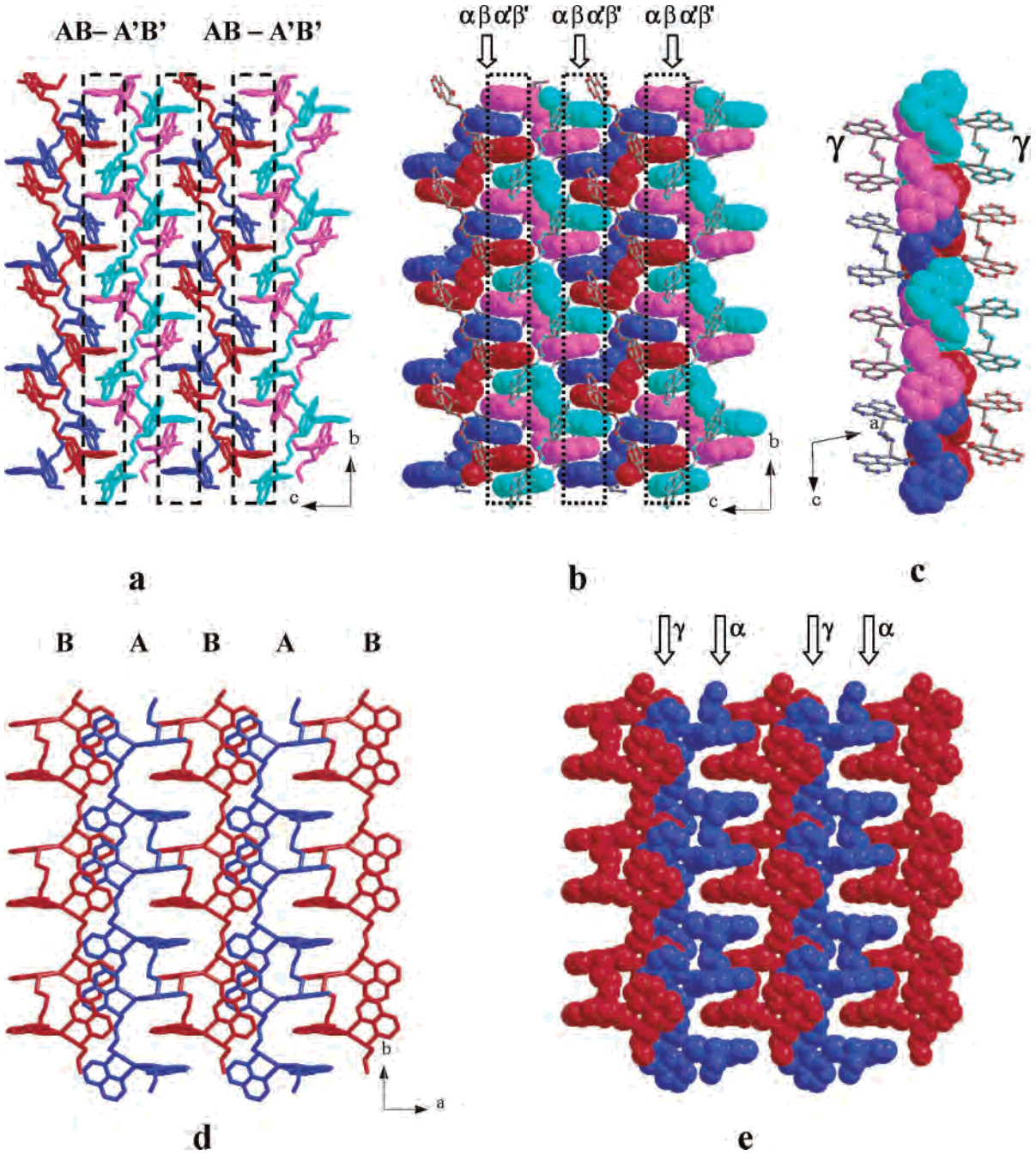

Figure 14. The double layer AB−A′B′−AB−A′B′··· in *bc* plane in **4** (top): (a) four AB units form three stacked aromatic columns, which are highlighted by dashed rods; (b) the closely stacked aromatic sheet (in space-filling mode) formed in the middle of the double layers. Stacked aromatic columns with $\alpha\beta\alpha'\beta'$ repeating units are highlighted by dashed rods; (c) top view of the double layer showing the back-to-back conformational ligands on both sides (wire mode) to form γ interactions. The AB−AB−AB−AB··· (or A′B′−A′B′−A′B′−A′B′···) layer in *ab* plane in **4** (bottom): (d) wire mode showing repeating of AB units along *a* axis; (e) space-filling mode showing the α interaction related AB units connected via γ interactions in *a* direction. Color representation of each chain is the same as in Figure 13.

rings $Ag_2S_3C_3$ share Ag−S edges to extend the chain structure, whereas in **3**, two type of rings, eight-membered Ag_4S_4 and 14-membered $Ag_2S_4C_8$, share S−Ag−S edges to generate the chain structure. In contrast, the chain structures in **2** and **4** can be considered as "single" although two independent Ag atoms and ligands exist in **4**. Different coordination geometries were found, including square pyramidal in **1**, square planar in **2**, and tetrahedral in **3** and **4**. The same ligand forms different structures with different counteranions, indicative of the remarkable influence of the anion on the crystal structure. Because every ligand contains two TQ rings linked by flexible $(CH_2)_n$ spacers, $\pi-\pi$ aromatic stacking interactions represent the predominant force governing the crystal packing. In **1**, the intramolecular interactions make full use of the TQ rings to exclude any intermolecular interactions. **2** shows the very simple but highly efficient intermolecular interactions based on its well-shaped trapezoidal wave structure. By contrast, **3** and **4** exhibit complicated $\pi-\pi$ interaction modes, each containing a four-directional aromatic stacking feature to organize the

Table 3. $\pi-\pi$ Interactions[a] in Complexes **1**−**4**

rings Cg(I)−Cg(J)	*d*	τ	CgI_perp	CgJ_perp	symmetry code
			complex **1**[b]		
Cg(2)−Cg(1)	4.027(4)	18.33	3.898	3.830	$1-x, 1/2+y, 3/2-z$
Cg(2)−Cg(3)	3.873(4)	19.77	3.679	3.563	$1-x, -1/2+y, 3/2-z$
Cg(3)−Cg(4)	4.126(4)	21.37	3.929	3.969	$1-x, -1/2+y, 3/2-z$
			Complex **2**[c]		
Cg(1)−Cg(4)	3.537(4)	2.25	3.413	3.446	$3/2-x, -1/2+y, z$
Cg(2)−Cg(3)	3.539(4)	1.88	3.414	3.442	$3/2-x, 1/2+y, z$
Cg(3)−Cg(4)	3.766(4)	0.62	3.457	3.462	$3/2-x, -1/2+y, z$
			Complex **3**[d]		
Cg(1)−Cg(3)	3.738(2)	2.56	3.382	3.439	$1-x, -y, 1-z$
Cg(2)−Cg(2)	3.837(2)	0.02	3.380	3.380	$-1-x, 1-y, -z$
Cg(2)−Cg(4)	3.632(2)	2.62	3.350	3.335	$-1-x, 1-y, -z$
Cg(3)−Cg(3)	3.915(3)	0.02	3.398	3.398	$1-x, -y, 1-z$
			Complex **4**[e]		
Cg(1)−Cg(2)	3.574(5)	3.64	3.467	3.514	$-x, 1-y, 1-z$
Cg(3)−Cg(4)	3.692(5)	10.12	3.546	3.617	$x, 1/2-y, -1/2+z$
Cg(3)−Cg(5)	3.680(5)	11.42	3.594	3.366	$1-x, -y, 1-z$

[a] Cg(I) = ring number I; τ = dihedral angle between rings I and J (°); *d* = distance between ring centroids (Å); CgI_perp = perpendicular distance of Cg(I) on ring J (Å); CgJ_perp = perpendicular distance of Cg(J) on ring I (Å). Calculated using PLATON; Spek, A. L. *Acta Crystallogr.* **1990**, A*46*, C34. [b] Cg(1): N(1), C(1)−C(4), C(9); Cg(2): N(2), C(13), C(18)−C(21); Cg(3): C(4)−C(9); Cg(4): C(13)−C(18). [c] Cg(1): N(1), C(1)−C(5); Cg(2): N(2), C(17)−C(21); Cg(3): N(1), C(1)−C(5); Cg(4): C(13)−C(17), C(21). [d] Cg(1): N(1), C(1)−C(5); Cg(2): N(2), C(18)−C(22); Cg(3): C(4)−C(9); Cg(4): C(14)−C(18), C(22). [e] Cg(1): N(2), C(18)−C(22); Cg(2): C(4)−C(9); Cg(3): N(3), C(23)−C(26), C(31); Cg(4): N(4), C(36)−C(39), C(44); Cg(5): C(39)−C(44).

structure into a 3D network. The nature of this difference appears to be determined by the length of the $(CH_2)_n$ spacers. As depicted in Scheme 2, the $-CH_2CH_2CH_2-$ spacer has definite mirror symmetry passing through the central carbon atom, which dictates the simple but well-defined head-to-head conformation of the ligand. However, the longer $-CH_2CH_2CH_2CH_2-$ spacer may take either mirror symmetry-related cis- or 2-fold symmetry-related trans-conformation, i.e., two side carbon atoms adopt syn- or anti-conformation or any intermediate conformation between them. This leads to a facile flexibility of the ligand, manifested in various conformations such as head-to-tail, back-to-back, or tail-to-tail, which lead to the different aromatic stacking modes. Another effect is due to the gauche conformation[16b,d,23] preferred by S atoms, which makes the TQ rings "fold up" from the $(CH_2)_n$ backbone (except for the back-to-back conformation in **4**) to provide effective supramolecular recognition sites.

Spectroscopy. The presence of IR absorptions in the ranges 1489−1597 and 777−787 cm^{-1} for all complexes is indicative of the presence of the TQ ligands. The two peaks at 1273 and 1029 cm^{-1} in complex **2** are evidence for the free $CF_3SO_3^-$ anion,[24] whereas those in the ranges 1088−1092 and 621−628 cm^{-1} for complex **1** and **4** clearly indicate the free ClO_4^- anion.[25] Absorptions at 1272 and 1027 cm^{-1} for free $CF_3SO_3^-$ are also found in complex **3**, together with a strong band at 1239 cm^{-1}, indicative of a second type of $CF_3SO_3^-$ anion whose coordination behavior, however, cannot be unambiguously assigned. The presence of CH_3CN in complex **3** is indicated by a weak absorption at 2298 cm^{-1}.

Table 4. ^{1}H NMR Data for C3TQ, C4TQ, and Complexes **1**−**4** in DMSO-d_6

	Chemical Shift (ppm)							
complex	H_1	H_2	H_3	H_4	H_5	H_6	H_7	H_8
C3TQ	8.89	7.46	8.34	7.70	7.57	7.59	3.26	2.14
1	8.96	7.56	8.47	7.84	7.65	7.88	3.28	2.08
2	8.96	7.57	8.48	7.85	7.65	7.89	3.28	2.07
C4TQ	8.89	7.57	8.36	7.70	7.57	7.57	3.13	1.95
3	8.99	7.65	8.54	7.97	7.70	7.98	3.17	1.82
4	8.96	7.62	8.49	7.90	7.66	7.86	3.15	1.85

	Coupling Constant (Hz)					
	$^3J(H^1H^2)$	$^4J(H^1H^3)$	$^3J(H^2H^3)$	$^3J(H^4H^5)$	$^3J(H^5H^6)$	$^3J(H^7H^8)$
C3TQ	4.0	1.5	8.5	8.0	7.5	7.0
1	4.0	1.5	8.3	8.0	8.0	7.0
2	4.0	1.5	8.0	8.0	8.0	7.0
C4TQ	4.0	1.5	8.0	7.8	8.0	7.0
3	4.0	1.5	8.3	8.0	8.0	6.3
4	4.0	1.5	8.0	8.0	8.0	6.3

Scheme 4

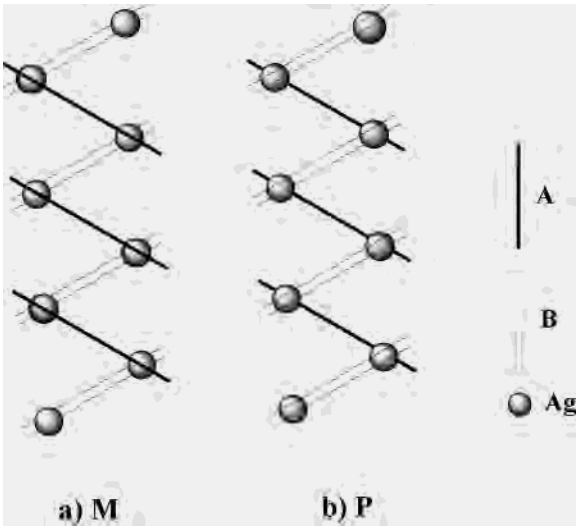

^{1}H NMR spectra of the ligands C3TQ, C4TQ, and the complexes **1**−**4** were recorded at room temperature in DMSO-d_6 solvent. The coordination of C3TQ or C4TQ to the Ag(I) ions results in a set of well-resolved signals which is shifted relative to those of the free ligands as exemplified in Figure S2. The chemical shifts and coupling constants are listed in Table 4. Coupling constants ^3J and ^4J in the ranges 4−8 and 1−1.5 Hz conform to the normal values for ortho and meta protons, respectively, similar to those previously reported for C6OQ[16a] (1,6-bis(8-oxaquinolyl)-hexane), OETQ[16b] (1,5-bis(8-thioquinolyl)-3-oxapentane), and ODTQ[16b] (1,8-bis(8-thioquinolyl)-3,6-dioxaoctane). Generally, the protons on the quinoline ring show a significant downfield shift for the complexes as compared with those of the free ligands. One finds that the coordination of the ligand also induced a downfield shift for the protons nearest to the sulfur atoms in the alkyl spacers, which is different from those OQ-based ligands and their complexes[16b] where

(24) (a) Johnston, D. H.; Shriver, D. F. *Inorg. Chem.* **1993**, *32*, 1045. (b) Huang, W.; Frech, R.; Wheeler, R. A. *J. Phys. Chem.* **1994**, *98*, 100. (c) Su, C.-Y.; Kang, B.-S.; Du, C.-X.; Yang, Q.-C.; Mak, T. C. W. *Inorg. Chem.* **2000**, *39*, 4843.

(25) (a) Agarwal, R. K.; Sarin, R. K. *Polyhedron* **1993**, *19*, 2411. (b) Pettinari, C.; Marchetti, F.; Polimante, R.; Cingolani, A.; Portalone, G.; Colapietro, M. *Inorg. Chim. Acta* **1996**, *249*, 215.

Scheme 5

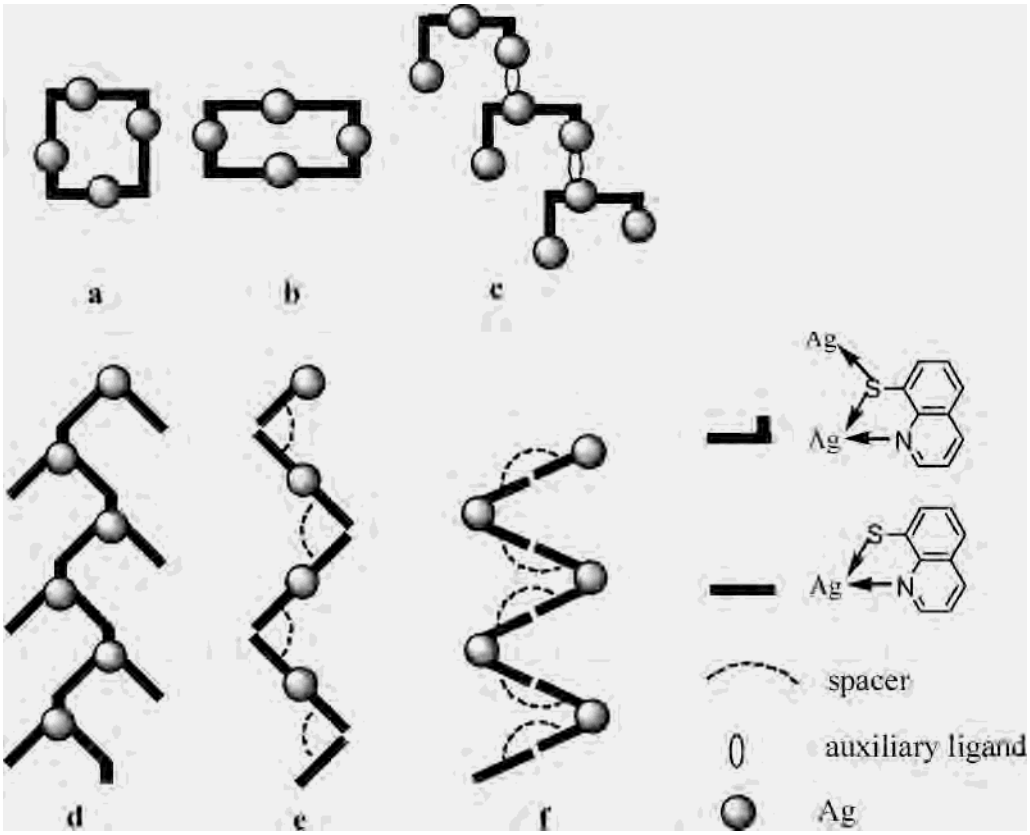

the alkyl protons in C6OQ are shifted upfield on coordination.

Conclusion

This work demonstrated that flexible bis-thioquinolyl ligands are a series of useful chelators in the construction of new supramolecular polymers containing silver(I) ions. As shown in Scheme 5, the TQ moiety often has two different coordination modes: non-sulfur bridging and sulfur bridging. The bridging mode provides for a variety of connection modes between two metal atoms. As a result of this, the sulfur-bridging TQ ligands have been successfully used to assemble many unique structures, depending upon the arrangement of the TQ moieties as demonstrated in Scheme 5, such as a in **3**, b in $[Ag_4(ODTQ)_2(\eta^1\text{-}NO_3)_2(\eta^2\text{-}NO_3)_2]$[16b] and $[Ag_4(OETQ)(ODTQ)(\eta^1\text{-}NO_3)_2(\eta^2\text{-}NO_3)_2]$,[16b] c in $[Ag_3(OETQ)(NO_3)_3]_n$,[16d] and d in **1** and $\{[Ag(C3TQ)](NO_3)\}_n$.[13e] The non-sulfur-bridging TQ ligands often form helicates by chelating a Ag(I) ion, such as e in **2** and f in **4**, $[Ag(m\text{-}XYTQ)]_n(ClO_4)_n$,[17b] and $[Ag(m\text{-}XYTQ)]_n(BF_4)_n$[17b] (*m*-XYTQ = α,α′-bis(8-thioquinolyl)-*m*-xylene).

The present study also indicates the following general trends that are particularly prevalent for type Ib ligands (Scheme 1): (1) TQ rings provide potential supramolecular interaction sites for $\pi-\pi$ aromatic stacking interactions, which are important forces in the construction of supramolecular networks. (2) The sulfur atoms play significant roles in increasing the coordination modes of the ligands by folding at the S site and increasing the coordination numbers of the Ag atoms. (3) The flexible spacer chains, assisted by the sulfur atoms, dictate the orientation of the TQ rings, resulting in diversified aromatic stacking interaction modes. (4) Other weak interactions such as C−H···O, Ag···S, and Ag···O also contribute to the stability of the supramolecules. In addition to the effect of the ligands on the construction of new supramolecules, the anions play important roles: the more polar triflate will sometimes coordinate to Ag(I) ions, such as in **3**, thereby completely changing the coordination environment of the Ag(I) ions, whereas the perchlorate anion is mostly free, although both interact weakly with cationic chains through the oxygen atoms.

Acknowledgment. This work was supported by the Natural Science Foundation of China and RFDP of Higher Education of China. Acknowledgment is made to the donors of the Petroleum Research Fund, administered by the American Chemical Society, for partial support through grant PRF #36822. C.Y.S. thanks the Alexander von Humboldt Foundation for a research fellowship.

Supporting Information Available: 2D layers in **3** formed via $\pi-\pi$ interactions in the *ab* and *ac* planes and partial ^{1}H NMR spectra of the ligands C3TQ, C4TQ, and the complexes **1**−**4** in DMSO-d_6 (PDF). X-ray crystallographic files for all structures (CIF). This material is available free of charge via the Internet at http://pubs.acs.org.

IC0341035